NUKLEONIKA 2013;58(1):245–250

ORIGINAL PAPER

Positron annihilation studies of mesoporous iron modified MCM-41 silica

Marek Wiertel,
Zbigniew Surowiec,
Mieczysław Budzyński,
Wojciech Gac

Abstract. MCM-41 silica materials modified by iron incorporation in the stage of its synthesis were investigated. The aim of the studies was determination of the nature of iron species and the influence of its content on the structural changes of materials and following the changes of their properties. For this purpose, the N_2 sorption/desorption method and positron annihilation lifetime spectroscopy (PALS) were used. Disappearance of the longest-lived *ortho*-positronium (*o*-Ps) component (τ_5) present in the PALS spectra of the initial MCM-41 material in the spectra of Fe-modified MCM-41 measured in vacuum is a result of a strong chemical *o*-Ps quenching and/or the Ps inhibition mechanism. Filling of pores by air or N_2 at ambient pressure causes reappearance of the (τ_5) component with lifetime shortened in comparison to that observed in vacuum for pure MCM-41 to the extent which can be explained by usual paramagnetic quenching in air. In contrary to the tendency observed for (τ_5) lifetime which is practically independent of Fe content, the relevant intensity I_5 monotonically decreases. This fact suggests that only inhibition of Ps formation occurs for the samples in air. Observed anti-quenching effect of air seems to be a result of competition of two processes: neutralization of surface active centres acting as inhibitors and considerably weaker paramagnetic quenching by O_2 molecules.

Key words: iron • MCM-41 silica mesoporous materials • N_2 sorption • positron annihilation • positron lifetime spectra

M. Wiertel✉, Z. Surowiec, M. Budzyński
Maria Curie-Skłodowska University,
Institute of Physics,
1 M. Curie-Skłodowskiej Sq., 20-031 Lublin, Poland,
Tel.: +48 81 537 6220, Fax: +48 81 537 6191,
E-mail: marek.wiertel@umcs.lublin.pl

W. Gac
Maria Curie-Skłodowska University,
Faculty of Chemistry,
3 M. Curie-Skłodowskiej Sq., 20-031 Lublin, Poland

Received: 25 July 2012
Accepted: 11 October 2012

Introduction

Recently, fuel cells have found wide interests. A significant barrier of widespread application of H_2-air polymer-electrolyte-membrane fuel cells, e.g. for vehicles or mobile devices is their costs. It is very important from technological and economical points of view to replace expensive heterogeneous electrocatalysts based on noble metals with those much cheaper based on transition metal oxides. Reduction of their cost will encourage widespread use of fuel cells. Several research papers reported that iron based cathodes showed a good performance [11, 12]. However, the main disadvantage was their relatively low volumetric activity compared with those Pt-based. In this aspect strongly dispersed iron oxide species, embedded in porous templates such as MCM-41 or obtained with that material via nanocasting techniques, seems to be very promising [1]. Highly ordered mesoporous MCM-41 silica is characterized by uniform pore diameter distribution, large total pore volume and large specific surface area [3]. Volume/surface concentration of active centres is one of a great importance parameter in heterogeneous catalytic systems. Such parameters are closely related to the structure of materials. Free-volume structure in them is represented by pores along with specific

vacancy-type defects within individual crystalline grains and intergranual boundaries. Better understanding of the processes of structural changes caused by incorporation different species to MCM-41 silica and factors influencing on stability of the obtained nanostructures is crucial for making further progress in development of new functional materials. Nitrogen adsorption/desorption (N_2 A/D) measurements or mercury porosimetry [5] have been widely used for the determination of porous structure of different class of materials for several years. Positron annihilation lifetime spectroscopy (PALS) is an additional, universal nowadays method to study pores and extended positron-trapping defects in solids despite their structural hierarchy. In any medium, the intrinsic lifetime of *ortho*-positronium (*o*-Ps) is reduced from 142 ns by the process called pick-off annihilation. The pick-off annihilation rate and, hence, the *o*-Ps lifetime are dependent on the size of the pore in which the positronium is trapped. Thus, *o*-Ps can be used as a porosimetric probe to evaluate the average sizes in the approximate range from a few tenths of a nanometer to 100 nm and to determine size distributions. If the pores are partially or completely filled by some material or material of walls, modified by introducing some chemical species, *o*-Ps living in localized states long enough can undergo various processes, e.g. chemical reactions, scattering on paramagnetic molecules and interaction with magnetic fields. As a result of those interactions, the pick-off lifetime of *o*-Ps may be further shortened. Relevant processes are called chemical quenching, paramagnetic quenching (or *ortho-para* conversion) and magnetic quenching, respectively [13]. Chemical reactions with the so-called inhibitors lead to Ps formation inhibition and have an effect on values of *o*-Ps lifetime components intensities. Chemical active centres scavenging electrons, positrons, holes etc. also act as inhibitors. All the phenomena enumerated above may potentially give valuable information on the structural and chemical properties of micro- and mesoporous materials [10].

The aim of the presented investigations was to give information about micro- and mesoscopic pore structure in Fe modified MCM-41 mesoporous silica. The purpose of this work was also to check the possibility of using PALS method to the quantitative characterization of internal structure of such materials in micro-scale.

Experimental

Iron silica mesoporous materials (Fe-MCM-41) were obtained by the application of a direct hydrothermal method. Hexadecyltrimethylammonium bromide (C16TAB) surfactant was dissolved in distilled water, and then suitable amounts of iron nitrate were introduced. Next, tetraethylorthosilicate (TEOS) was slowly added to the mixture while stirring. The pH of the solution was slowly increased by the introduction of ammonium hydroxide. The mixture was stirred for 1 h. The obtained product was filtered, washed with distilled water, dried overnight at 90°C and calcined in air at 550°C for 6 h in order to remove surfactants and to perform transformation of the precursors. The introduced amounts of iron were varied, in order to obtain samples containing 3.0 wt.% (denoted as Fe-MCM-41(A)), 6.5 wt.% (Fe-MCM-41(B)), 12.5 wt.% (Fe-MCM-41(C)) and 24.3 wt.% (Fe-MCM-41(D)).

The porous structure of materials was determined by the analysis of the nitrogen adsorption/desorption isotherms obtained volumetrically at 77 K using an ASAP 2405N apparatus (Micromeritics Co, USA). Samples before measurements were outgassed (under $\sim 10^{-2}$ Pa) at 200°C. The adsorption data were used to evaluate BET (Brunauer-Emmet-Teller) specific surface area, S_{BET} (from the linear BET plots). The mesoporous structure was characterized by the distribution function of mesopore volume and average pore diameter (APD) calculated by applying the standard Barrett-Joyner-Halenda (BJH) method [2]. APD is defined as $4V/S$, where V is the BJH cumulative adsorption pore volume of pores between 1.7 and 100 nm, and S is the BJH cumulative adsorption surface area of pores in the same range.

In PALS measurements the ^{22}Na positron source sealed in a Kapton envelope was placed between two layers of the powder sample, pressed together by a screwed cap inside a small copper container. This assembly was placed in a vacuum chamber allowing obtaining a pressure better than 0.01 Pa. Positron lifetime spectra were recorded at room temperature, using a fast-slow coincidence spectrometer with pulse pile-up inspection. The spectrometer, equipped with two scintillation counters, consists of BaF_2 coupled to XP2020Q photomultiplier tubes. The geometry excluding the possibility of summing effects was used [6]. In porous media an essential number of *o*-Ps atoms decay into 3 gamma-quanta. Their energy spectrum is continuous, extending from 0 to 511 keV. Thus, to improve the efficiency of counting the stop energy window in the spectrometer was widely open (80% of the energy range). At such a setting the resolution time was 0.29 ns (for a ^{60}Co source with a ^{22}Na window). The time base of the PALS setup was 2 μs (16 384 channels). The total counts were 3×10^7 or 10^8 for each spectrum measured in vacuum or in air, respectively. The positron lifetime spectra were analyzed using the LT program [9]. A source component 0.382 ns (annihilation in 8 μm Kapton foil) of intensity of about (11÷12)% was taken into account in lifetime data processing.

Results and discussion

The porous structure and surface properties of the materials modified with small amounts of iron were similar to those of MCM-41 pure silica mesoporous support. These samples showed large surface area (S_{BET}) exceeding 1000 m^2/g (Fig. 2). The shape of the adsorption/desorption isotherms (Fig. 1) for the Fe-MCM-41(A) sample indicated the formation of regular mesopores with a mean pore diameter (w_d) of about 3.3 nm. A small and flat hysteresis loop can be observed in the range of relative pressures ranging from 0.5 to 0.8. This effect can indicate the presence of the some irregularities in the structure of silica mesoporous material, connected with the development of bottle-ink type pores. Structure changes caused by incorporation of iron are a reason for N_2 diffusion restrictions in silica pores influencing the shape of N_2 isotherms.

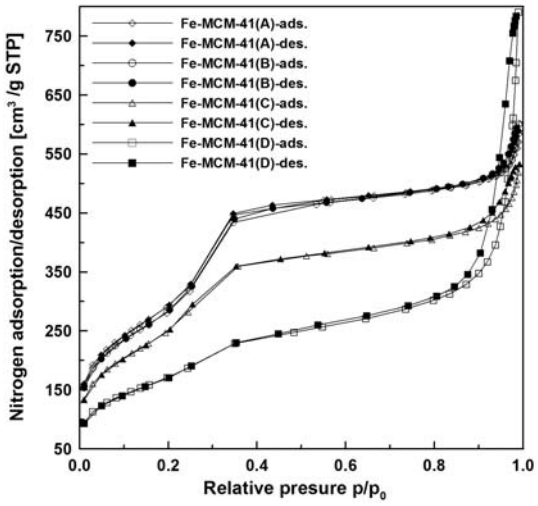

Fig. 1. N_2 adsorption/desorption isotherms for MCM-41--suported Fe-based catalysts. For the sample labels explanation and Fe content see Table 1.

An increase of metal concentration induces distortion of the well-ordered structure and a decrease of the total surface area of the samples. The typical step on the isotherms at 0.3 of p/p_0 becomes less pronounced, and finally disappears for the Fe-MCM-41(D) sample. While the hysteresis loop at higher relative pressures is developed and shifts to higher relative pressures. These effects result from the transformation of the regular channels to the worm-like, more open structures and formation of macropores. The shape of the isotherm for the Fe-MCM-41(D) may indicate the presence of slit-like pores. In our opinion such effects are connected with distortion of the micellar structures of surfactant molecules caused by the introduction of large amounts of ionic species and their transformation to the oxide nanoparticles located in the as-prepared silica pores and embedded within the silica walls. In Fig. 2 pore sizes distributions (PSDs) are shown. The captions in this figure give the average pore diameter values calculated by the BJH method from adsorption isotherms.

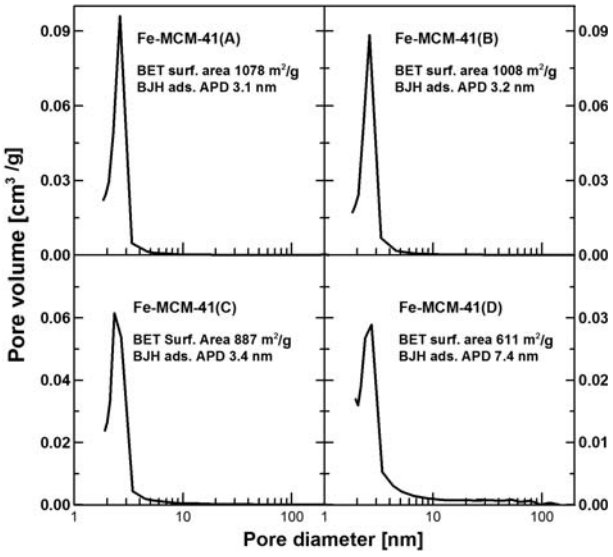

Fig. 2. Pore size distributions determined from adsorption/desorption isotherms of the investigated samples by BJH method. APD – average pore diameter obtained by BJH method from N_2 adsorption.

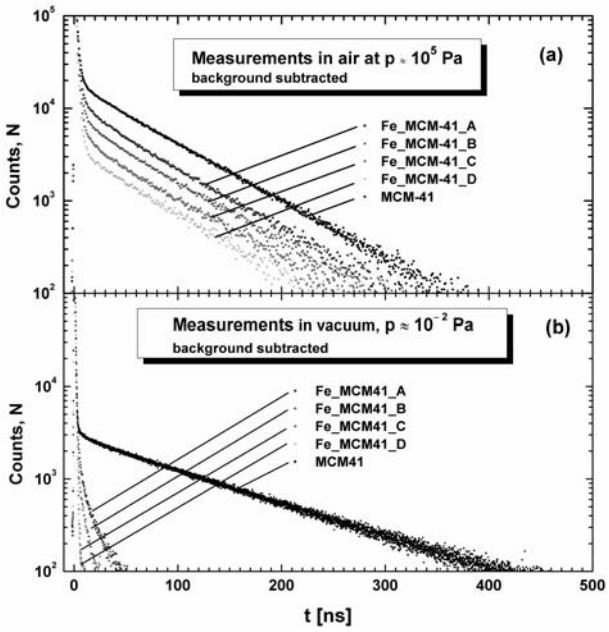

Fig. 3. Positron annihilation lifetime spectra of four Fe--MCM-41 samples measured in air (a) and in vacuum (b) normalized to time of measurement.

Before starting the actual positron annihilation lifetime (PAL) measurements, the dynamic of degasing and sorption processes was studied by observing time evolution of one-hour spectra. For the Fe modified MCM-41 samples, dynamic equilibrium state had been achieved after about 6 h from switching on a vacuum pump removing air or pure gaseous N_2. After filling of the measuring chamber with N_2, equilibrium state had been reached after about 12 h.

Four different PAL spectra for the investigated samples measured in vacuum (a) and in air at ambient pressure (b) are shown in Fig. 3. The intensities of the longest-lived component (τ_5) measured in air systematically decreases along with increasing Fe content in the samples. Simultaneously, one can observe disappearance of this component in measurements in vacuum (see Fig. 5). Detailed values of lifetimes and intensities of *ortho*-positronium (*o*-Ps) components are given in Table 1. The spectra are relatively complicated. In the fitting procedure it was finally assumed that they consist of five discrete exponential components: two of them are very short-lived, the first belonging, in principle, to the intrinsic decay of *para*-positronium (*p*-Ps, $\tau_1 \approx$ 0.13 ns) and the second one is related to the annihilation of free positrons (e^+, $\tau_2 \approx 0.45$ ns). The latter component on the one hand origins from annihilation of free positrons trapped in vacancy clusters formed in iron oxide nanoparticles or on their surfaces [4], on the other hand from positron annihilation in small structural cages in amorphous silica walls, for instance, tetrahedrally coordinated Si/Fe monovacances in $[V_{Si/Fe}O_{4/2}]^-$ basic structural blocks. As you can see, these lifetimes are only approximations of several undistinguishable components comparable to the time resolution of the measuring system. The τ_1 parameter was fixed in the fitting procedure in order to obtain reasonable standard deviations for the parameters of long-lived *o*-Ps components. The component (τ_2) seems to be essential in the further considerations. Its lifetime value remains constant but

Table 1. The lifetimes and intensities of *o*-Ps components measured in vacuum ($p \approx 0.01$ Pa) and in air (ambient pressure) for MCM-41 and Fe modified MCM-41 samples

Sample		τ_3	τ_4	τ_5	I_3	I_4	I_5
		(ns)			(%)		
Pure MCM-41	vacuum	4.10(49)	40.9(1.5)	125.13(55)	0.43(11)	1.13(28)	24.16(32)
	air	2.00(11)	22.84(61)	70.81(25)	7.99(27)	1.00(11)	16.80(21)
Fe-MCM-41(A)	vacuum	2.49(27)	10.46(76)	41.2(1.1)	1.35(13)	0.85(11)	0.82(17)
3.0 wt.% Fe	air	1.95(10)	13.87(49)	67.50(31)	6.08(22)	0.98(8)	7.67(16)
Fe-MCM-41(B)	vacuum	0.98(18)	18.13(60)	not obs. [a]	3.95(61)	0.46(9)	not obs. [a]
6.5 wt.% Fe	air	1.94(9)	13.26(51)	68.26(36)	6.70(21)	0.46(9)	5.49(13)
Fe-MCM-41(C)	vacuum	1.35(31)	10.79(73)	not obs. [a]	0.84(41)	0.11(7)	not obs. [a]
12.5 wt.% Fe	air	1.90(11)	10.75(50)	68.95(38)	4.64(20)	0.56(7)	3.70(12)
Fe-MCM-41(D)	vacuum	2.30(39)	37.83(98)	not obs. [a]	0.20(15)	0.21(6)	not obs. [a]
24.3 wt.% Fe	air	1.78(13)	6.45(54)	64.67(36)	4.17(20)	0.32(13)	2.71(11)
	N_2	2.65(38)	13.95(70)	77.07(51)	0.28(8)	0.33(7)	1.96(14)

[a] not observed.

its intensities changes from about 42% in pure MCM-41 to 67% in the sample with a maximum Fe content measured in air and from 30 to 73% in vacuum, respectively. This can be explained as follows. Along with increasing Fe content, the numbers of Fe atoms isomorphously substituted in the tetrahedral sites in the centre of the $[FeO_4/_2]^-$ units embedded into the structurally similar net of $[SiO_4/_2]^-$ tetrahedral in amorphous SiO_2 (framework sittings) and amount of Fe in the form of iron oxide nanocrystallites, deposited mainly on surfaces of MCM-41 walls (extra-framework locations) increases. As a result of interaction between free positrons and Fe-modified silica walls and nanocrystallites relative contribution of free annihilation component I_2 to the total annihilation process significantly augments (by about 25% in air and ca. 43% in vacuum) due to increasing probability of free positron annihilation in media enriched in excess electrons. This is reflected in the data on intensities of *o*-Ps components collected in Table 1. The sum $I_{o\text{-Ps}} = I_3 + I_4 + I_5$ for the measurements performed in air adequately diminishes. In the case of measurements in vacuum this sum decreases almost to the same extent at the expense of the total *o*-Ps contribution and the first component. It can be also remembered that typical lifetimes of positron in e^+-molecule complexes are about (0.4÷0.5) ns [8].

Besides the two components discussed above, in the investigated samples of Fe-MCM-41 three long-lived *o*-Ps components were observed in the positron lifetime spectra. The shortest-lived among them (τ_3) is difficult to unique interpretation. This component probably arises owing to the pick-off annihilation of *o*-Ps formed in the some kind of open-volume defects on the surfaces of amorphous silica walls. The experimentally confirmed high sensitivity of I_3 and τ_3 to the presence of gases filling free spaces in the samples and/or their adsorption on the samples surfaces support such an interpretation. The medium-lived one (τ_4) results from the decay of *o*-Ps trapped inside of nanopores and the longest-lived among them (τ_5) is related to the pick-off annihilation of *o*-Ps trapped in free volume in intergranular spaces of the material [16]. The *o*-Ps lifetimes and their intensities changes with increasing Fe content for the Fe-MCM-41 samples in air under ambient pressure are presented in Fig. 4. The values of lifetimes remain principally constant within error limits with the exception of that for τ_4 which slightly decreases. For the same samples also the measurements in an evacuated measuring chamber were performed and their results are collected in Table 1. The τ_4 first decreases remarkably and then it changes irregularly. In the Fe-MCM-41(D) sample this component achieves a value almost equal to τ_4 in empty MCM-41. The systematic decrease of τ_4 and I_4 measured in air suggests that the probability of an escape of *o*-Ps trapped in primary silica nanochannels increases. It is correlated with the bottle-ink and slit-like pores formation hypothesis accepted from N_2 A/D measurements. The lifetime τ_5 in the evacuated samples rapidly decreases and this component is not observed at a Fe content larger than 3 wt.%. Entirely different dependences on Fe content were observed for measurements in air. The τ_5 slightly decreases (Fig. 4) and I_5 monotonically diminishes. A main contribution to I_5 is caused by Ps atoms escaping from primary pores to inter-granular spaces. The process of Ps escape in

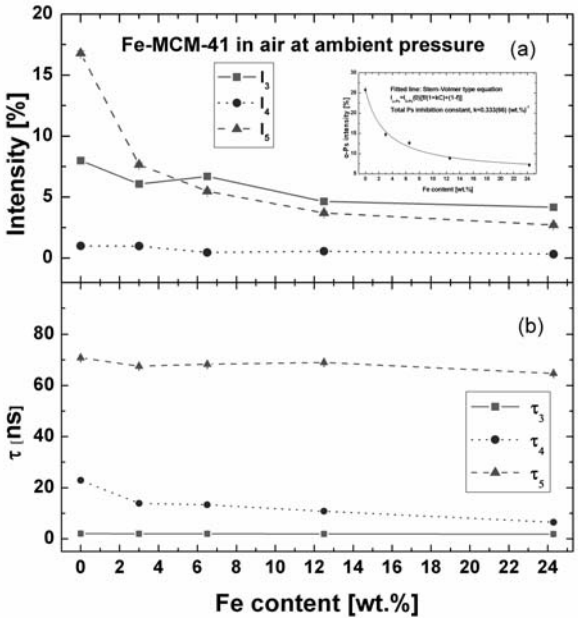

Fig. 4. The dependences of intensities (a) and lifetimes (b) of the three *o*-Ps components on Fe content for the Fe-MCM-41 silica materials measured in air at room temperature. Inset in panel (b) shows fitted to the dependence of total *o*-Ps intensity on Fe content Stern-Volmer type equation valid for the case of partial inhibition.

empty MCM-41 can be characterized by escape rate λ_{esc} defined as:

$$\lambda_{esc} = 1/\tau_4 - \lambda_{o\text{-Ps}}(Rp) \quad (1)$$

where: τ_4 – lifetime of *o*-Ps inside in the primary silica pores; $\lambda_{o\text{-Ps}}(Rp)$ – pick-off annihilation rate determined from the extended Tao-Eldrup model for cylindrical shape of pores [15, 17] with pore radius R_p, and R_p is a pore radius at the peak of PSD obtained by the BJH method from N_2 adsorption isotherms. In empty MCM-41 from τ_4 measured in vacuum and R_p = 1.32 nm λ_{esc} estimated from formula (1) is equal to 2.48(39) μs^{-1}. Besides, it is known from other investigations that in nanocomposite material Fe-MCM-41 an amount of Fe which can be substituted for Si in amorphous SiO_2 walls is limited to about 1.1 wt.% [14]. The remaining part of iron forms nanoclusters or nanocrystallites of iron oxide species. Interactions between Ps atoms and Fe^{3+} oxidization agents located on nanocluster surfaces causes chemical quenching of Ps. It is not excluded that these Fe^{3+} ions, built into silica framework, play a role of inhibitors. The observed in air value of the τ_5 lifetime and its relatively large intensity of the order of a few per cent can be explained as follows. Physisorption of small amounts of the gas molecules on the pore surface increases the *o*-Ps lifetime, due to neutralization of chemically active sites on the oxide nanoclusters surfaces causes that the chemical quenching becomes ineffective. In the case of the investigated samples, probably a coating of Fe_2O_3 deposits by monolayer of predominantly N_2 molecules from air takes place. Additionally, the monolayer gives a film thick enough to isolate oxide species with much lower electron density layer. Paramagnetic quenching O_2 molecules by present in air is compensated in excess by switching off chemical quenching. This effect gives opposite and predominating result to an *o*-Ps to *p*-Ps conversion in interaction with paramagnetic air oxygen molecules.

In the inset to Fig. 4a the dependence of the $I_{o\text{-Ps}}$ on Fe content is shown. The empirical Stern-Volmer type formula valid for the case of partial inhibition [7]:

$$I_{o\text{-Ps}}(C) = I_{o\text{-Ps}}(0)\,[f/(1 + k \cdot C) + (1 - f)] \quad (2)$$

has been used to fit a curve of *o*-Ps yield $I_{o\text{-Ps}}$ as a function of Fe inhibitor concentration C. In this equation $I_{o\text{-Ps}}(0)$ is *o*-Ps yield in pure MCM-41and f is an inhibited fraction. From this fitting, a value of the partial inhibition rate constant k = 0.333(66) $(wt.\%)^{-1}$ was determined. Because from data in Table 1 it can by deduced that an averaged lifetime of *o*-Ps component practically is constant in all the samples measured under air at atmospheric pressure, it is believed that only the *o*-Ps inhibition effect related to Fe additives occurs. An "external" air quenching has been taken into account by the assumption in Eq. (1) $I_{o\text{-Ps}}(0)$ equal to its value in pure MCM-41 in air.

Lifetime τ_5 observed in Fe-MCM-41 composite in air is only somewhat smaller than the value observed for pure MCM-41 (Table 1). It indicates that intergranular spaces are of similar size in all samples.

Conclusions

The PALS method cannot be used in a simple way to determine pore sizes in Fe modified MCM-41 samples because of the occurrence of many disturbing factors, e.g. a very strong chemical *o*-Ps quenching, paramagnetic quenching, Ps escaping from pores and not precisely determined the influence of Fe content on structural changes. The adsorption of air molecules on the nanocrystallites surfaces eliminates an immediate interaction between *o*-Ps atoms and located on them active centres and, as a consequence, a raise of the long-lived *o*-Ps lifetime components. The observed anti-quenching effect is a result of competition of two phenomena: practically switching off a pick-off mechanism related to the interaction of *o*-Ps with chemical species occurring in Fe modified mesoporous silica and considerably weaker paramagnetic quenching by oxygen molecules. An unambiguous and detailed explanation of Ps-inhibition mechanism needs further investigations and hence the presented results may not be conclusive.

References

1. Arends IWCE, Sheldon RA (2001) Activities and stabilities of heterogeneous catalysts in selective liquid phase oxidations: recent development. Appl Catal A 212:175–187
2. Barrett EP, Joyner LG, Halenda PP (1951) The determination of pore volume and area distribution in porous substances. Computations from nitrogen isotherms. J Am Chem Soc 73:373–380
3. Beck JS, Vartuli JC, Roth WJ *et al*. (1992) A new family of mesoporous sieves prepared with liquid crystal templates. J Am Chem Soc 114:10834–10843
4. Chakrabarti S, Chaudhuri S (2005) Positron annihilation lifetime changes across the structural phase transition in nanocrystalline Fe_2O_3. Phys Rev B 71:064105 (6 pp)
5. Giesche H (2006) Mercury porosimetry: a general (practical) overview. Part Part Syst Char 23:9–19
6. Goworek T, Górniak W, Wawryszczuk J (1992) The sources of distortions and errors in the analysis of positron lifitime spectra. Nucl Instrum Methods A 321:560–570
7. Ito Y (1988) Radiation chemistry: Intraspur effects and positronium formation mechanisms. In: Schrader DM, Jean YC (eds) Positron and positronium chemistry. Elsevier, Amsterdam, pp 120–158
8. Jean YC, Schrader DM (1988) Experimental techniques in positron and positronium chemistry. In: Schrader DM, Jean YC (eds) Positron and positronium chemistry. Elsevier, Amsterdam, pp 91–119
9. Kansy J (1994) Microcomputer program for analysis of positron annihilation lifetime spectra. Nucl Instrum Methods A 374:235–244
10. Kobayashi Y, Ito K, Oka T, Hirata K (2007) Positronium chemistry in porous materials. Radiat Phys Chem 76:224–230
11. Lefèvre M, Proietti E, Jaouen F, Dodelet JP (2009) Iron-based cathode catalyst with enhanced power density in polymer electrolyte membrane fuel cells. Science 324:71–74
12. Proietti E, Jaouen F, Lefèvre M *et al*. (2011) Iron-based cathode catalyst with enhanced power density in polymer electrolyte membrane fuel cells. Sci Commun 2, Article no. 416
13. Schrader DM, Jean YC (1988) Introduction. In: Schrader DM, Jean YC (eds) Positron and positronium chemistry. Elsevier, Amsterdam, pp 1–26

14. Wang Y, Zhang Q, Shishido T, Takehira K (2002) Characterizations of iron-containing MCM-41 and its catalytic properties in epoxidation of styrene with hydrogen peroxide. J Catal 209:186–196
15. Zaleski R (2010) EELViS, http://eelvis.sourceforge.net
16. Zaleski R, Wawryszczuk J, Borówka A, Goworek J, Goworek T (2003) Temperature changes of the template structure in MCM-41 type materials; positron annihilation studies. Microporous Mesoporous Mater 62: 47–60
17. Zaleski R, Wawryszczuk J, Goworek T (2007) Pick-off models in the studies of mesoporous silica MCM-41. Comparison of various methods of the PAL spectra analysis. Radiat Phys Chem 76:243–247